

## Short-term synaptic dynamics promote phase maintenance in multi-phasic rhythms

Yair Manor<sup>1</sup>, Victoria Booth<sup>2</sup>, Amitabha Bose<sup>2</sup>, Farzan Nadim<sup>2,3</sup>.

1. Life Science Department and Zlotowski Center for Neurosciences, Ben-Gurion University of the Negev, Beer-Sheva, Israel 84105. 2. Department of Mathematical Sciences, NJIT, Newark, NJ 07102 and 3. Department of Biological Sciences, Rutgers University, Newark, NJ 07102

### Abstract

We show that in an inhibitory rhythmic network synaptic depression promotes phase constancy. As cycle period increases, the synapse recovers from depression and becomes more effective in delaying the postsynaptic cell. As a result, the delay between the pre- and postsynaptic bursts increases as cycle period increases. We discuss the dependence of the bursting phase of the postsynaptic cell on the strength and kinetics of the depressing synapse.

### Introduction

Rhythmic activities are commonly produced over a wide range of cycle frequencies. Often, these rhythmic patterns involve activities of multiple units at different times within each cycle. When cycle frequency is altered, the time delay between two events may remain constant or it may change. Systems of the former type are latency-locked systems. Examples include terrestrial locomotion in bipeds and tetrapods (Grillner, 1981) and insects (Pearson and Iles, 1970), swimmeret beating in crayfish (Davis, 1969), pyloric-gastric interaction in crabs (Nadim et al., 1999) and uropod movements in sand crabs (Paul, 1971). In many systems, however the time intervals between different events change in proportion with the cycle period. Such systems are phase-locked systems, because the ratio of time latency and cycle period (i.e., phase) is maintained. Phase locking occurs in a variety of systems such as the Tritonia swim network (Hume et al., 1982), the pyloric rhythm of the spiny lobster (Hooper, 1997a, b) gill ventilation in the shore crab (Dicaprio et al., 1997; Young, 1975), lamprey swimming (Cohen et al., 1992; Williams, 1992) and leech swimming (Friesen and Pearce, 1993). Despite its importance in many motor pattern generators, the mechanism underlying phase maintenance is still unclear. Changes in the relative timings of events in a motor pattern may be caused by changes in intrinsic properties of the neurons, the strength of chemical synapses or electrical synapses. In this work we propose that short-term synaptic depression in inhibitory synapses play a pivotal role in promoting phase constancy. We illustrate this idea using a computational model consisting of an oscillator that makes an inhibitory synapse onto a follower cell. If the synapse is non-depressing, the postsynaptic cell always starts its burst at a fixed latency after the beginning of the presynaptic burst. Hence the phase between pre- and postsynaptic cell decreases as the cycle period increases. However, when the synapse shows depression, in some frequency range the interval between post- and presynaptic bursts increases as the cycle period increases. The increase in this interval is nearly proportional to the change in period and the phase is approximately constant. We discuss how the strength and kinetics of the depressing synapse affect the phase of the postsynaptic cell.

### The model

The model consists of an oscillator  $O$  and a follower cell  $F$ . The two cells  $i = \{O, F\}$  are modeled with standard current balance equations based on the Morris-Lecar model (Morris and Lecar, 1981):

$$(1) \quad V_i' = g_{L,i}(E_{L,i} - V_i) + \bar{g}_{K,i}w_i(E_{K,i} - V_i) + \bar{g}_{Ca,i}m_{\infty,i}(V_i)(E_{Ca,i} - V_i)$$

$$(2) \quad \tau_i(V_i)w_i' = w_{\infty,i}(V_i) - w_i$$

Where  $V_i$  is the membrane potential and  $w_i$  is a recovery variable. The cycle period of  $O$  can be modified by changing the time constant of the recovery process  $\tau_O$ . When  $V_O > V_{thresh}$ ,  $O$  is considered to be in the active state (or bursting) and  $\tau_O = T_R$ . Otherwise we consider that  $O$  is silent and  $\tau_O = T_L$ . Similar equations hold for  $F$ , with the same  $V_{thresh}$  but distinct time constants. We change the cycle period by changing  $T_L$ . This ensures that the duration of the active state of  $O$  does not change with period.

The parameters are chosen such that, without any synaptic input,  $F$  is at a high-voltage active state. The synaptic current from  $O$  adds an additional term to the left hand side of (1)

$$I_{O \rightarrow F} = g_{syn}s(V_F - E_{syn}),$$

where  $E_{syn}$  is the synaptic reversal potential,  $g_{syn}$  is the maximal synaptic conductance and  $s$  is a state variable that represents synaptic activation.

The dynamics of  $s$  depend on a variable  $d$ , which measures the level of depression of the synapse. When  $O$  is in the active state  $s$  and  $d$  obey the following set of equations:

$$(3) \quad d' = -d / \tau_\beta, \quad d(0) = d_0$$

$$(4) \quad s' = -s / \tau_\gamma, \quad s(0) = d_0,$$

for some initial value  $d_0$ . Note that the initial value  $s(0)$  is set to  $d_0$ . Let  $T_A$  be the burst duration of  $O$  and  $T_I$  be the interburst time of  $O$ . In the silent state of  $O$ ,

$$(5) \quad d' = (1-d) / \tau_\alpha, \quad d(T_A) = d_0 \exp(-T_A / \tau_\beta)$$

$$(6) \quad s' = -s / \tau_\kappa, \quad s(T_A) = d_0 \exp(-T_A / \tau_\gamma).$$

When  $O$  becomes active again, Equations 3 and 4 again hold except that  $s(T_I+T_A)$  is reset to be  $d(T_I+T_A)$ . Thus the synaptic variable  $s$  is set to the value of  $d$  exactly at the moment in time when  $O$  jumps to the active state. At all other moments in time, the two variables are decoupled. If  $O$  fires periodically, then  $d_0 = d(T_I+T_A)$  which can be rewritten as

$$(7) \quad d_0 = (1 - \exp(-T_I/\tau_\alpha)) / (1 - \exp(-T_I/\tau_\alpha) \exp(-T_A / \tau_\beta)).$$

This expression shows that the level of depression changes as a function of the interburst interval  $T_I$ , the burst duration  $T_A$  and of the depression ( $\tau_\beta$ ) and recovery ( $\tau_\alpha$ ) time constants.

If  $g_{syn}$  is sufficiently large and the synapse is strong ( $d_0$  is large), then the inhibitory synaptic current will prohibit  $F$  from firing until the synapse from  $O$  to  $F$  has decayed enough. Alternatively, if the synapse is weak ( $d_0$  is small) it will have a minimal effect on the activity of  $F$  and therefore the firing of  $F$  is governed by its intrinsic dynamics.

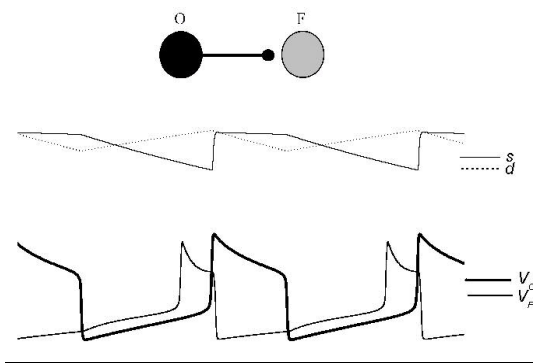


**Figure 1.** *The model.* An oscillator  $O$  and a follower cell  $F$  are connected via an inhibitory synapse from  $O$  to  $F$ . When the synapse is modeled as depressing, the synaptic conductance is the product of the maximal conductance and  $s$ . When  $O$  starts its burst,  $s$  is set to the value of  $d$ , which represents depression and recovery.

## Results

We will start by defining phase and will then show what parameters affect it. Let us assume that  $O$  begins its burst at  $t=0$  and has period  $P$ . Just prior to the burst of  $O$ ,  $F$  is at a high-voltage active state. The effect of  $O$ 's burst is to cause  $F$  to fall to its low-voltage silent state. At some later time, which we denote  $\Delta t$ ,  $F$  returns to the active state. Therefore the phase at which  $F$  fires with respect to the onset of  $O$ 's burst is  $\phi = \Delta t / P$ . To gain insight into what mechanisms promote phase constancy, it is crucial to understand what determines the firing time  $\Delta t$  of  $F$ .

Figure 2 shows a plot of  $\phi$  as a function of  $P$ . When the synapse was non-depressing (dotted curve),  $\phi$  decayed as  $P$  increases. At  $P = 250$ ,  $O$  and  $F$  started to burst at the same time ( $\phi = 1$ ). For  $P$  values lower than 250, the biphasic rhythm was disrupted and  $F$  remained continuously inhibited by  $O$ . In contrast, when the synapse was depressing (solid curve)  $\Delta t$  initially increased as  $P$  increased. In the case shown in Figure 2, for  $175 \leq P \leq 275$ , a change in  $P$  produced a larger change in  $\Delta t$  and hence  $\phi$  increased as  $P$  increased. We refer to the region where  $\phi$  increased as the hump. For other  $P$  values, a change in  $P$  produced a smaller change in  $\Delta t$  and hence  $\phi$  decreased as  $P$  increased. With very large

values of  $P$ , the synapse fully recovered during the interburst of  $O$ . Hence, a change in  $P$  did not produce any change in  $\Delta t$  and  $\phi$  decreased proportionally to  $1/P$ . When  $P$  was smaller than 150, the rhythm was disrupted.

Figure 2 illustrates two important points. (1) A depressing synapse, compared to a non-depressing synapse, minimizes the change in phase as period is modified. For example, in Figure 2 a 2-fold increase of period, from 250 to 500, yields a change of phase of 50% (from .98 to 0.49) for a non-depressing synapse and of 16% (from 0.86 to 0.72) for a depressing synapse. (2) A depressing synapse increases the period range for which  $F$  bursts. In Figure 2, the rhythm was disrupted ( $F$  did not burst) with  $P$  less than 150 for a depressing synapse but with a non-depressing synapse the disruption happened for  $P$  less than 250.

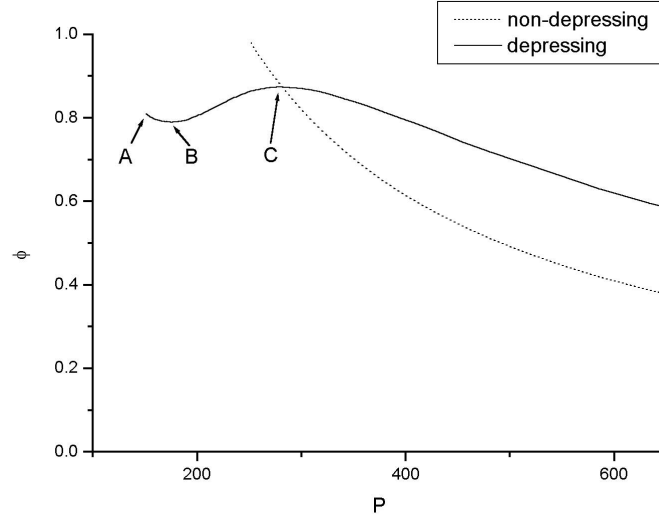


**Figure 2** Phase of  $F$  burst onset as function of cycling period. When the synapse is non-depressing (dotted line),  $\Delta t$  is fixed and the phase  $\phi$  decays as period  $P$  increases. For  $P < 250$ , the rhythm is disrupted. When the synapse is depressing,  $\Delta t$  increases as  $P$  increases. In the case shown, between  $P > 175$  (B) and  $P < 275$  (C)  $\Delta t$  increases more than  $P$ , and in that range  $\phi$  increases as  $P$  increases. For  $P < 150$  (A), the rhythm is disrupted.

The main result of this work that synaptic depression promotes phase constancy is dependent on the crucial, yet simple, fact that the firing time of  $F$  is a function of the strength of the synapse. The firing time is effectively determined by the value  $d_0$ , which gives a measure of the strength of the depressing synapse at the moment  $O$  begins its burst. The term  $d_0$  itself depends on two key factors: (1) the intrinsic dynamics of  $F$  as it evolves in its silent state, and (2) the decay time constant of inhibition  $\tau_k$ . However, as we shall discuss below, each of these factors may only be relevant in determining  $\Delta t$  for certain intervals of  $P$ .

If the synapse is weak, the firing of  $F$  is governed by its intrinsic dynamics, i.e.,  $\Delta t$  is mainly determined by the intrinsic time constant  $\tau_w$  of  $F$  during its silent state. In particular,  $\Delta t$  is largely independent of  $\tau_k$ . Moreover, as the period  $P$  increases, by increasing  $T_I$ ,  $\Delta t$  does not change much, since the firing time is intrinsically determined. Thus in the interval of periods between A and B in Figure 2,  $\phi$  behaves like  $1/P$ .

If the synapse is strong, the main parameter affecting  $\Delta t$  is  $\tau_k$  the time constant for the decay of inhibition when  $O$  is silent. Notice that this parameter was irrelevant to determining  $\Delta t$  in the prior case. Thus if  $\tau_k$  is large,  $\Delta t$  can increase very rapidly with small changes in  $P$  that make the synapse increase its strength. This observation accounts for the increase in phase observed between points B and C in Figure 2. As the period  $P$  becomes very large, the synapse can no longer be considered a depressing synapse, since it would recover fully during each interburst of  $O$ . Therefore the firing time  $\Delta t$  would become constant so that the phase behaves like  $1/P$ . This accounts for the behavior of the phase curve for  $P$  values to the right of C in Figure 2.

The key factor, thus, is the value of  $s$  and  $d$  at the beginning of the burst in  $O$  (Figure 1). If the synapse is not depressing, this value is independent of  $P$  and hence  $\Delta t$  is constant. However, if the synapse is depressing  $\Delta t$  becomes dependent on the cycle period: as the cycle period increases, there is a longer time during which  $d$  can recover and increase towards 1. Since  $s$  assumes the value of  $d$  at the beginning of the burst of  $O$ , as the cycle period increases  $s$  becomes larger, and as a result  $\Delta t$  increases. In addition, the intrinsic dynamics in  $F$  (the recovery variable  $W_F$ ) also play an important role, since these dynamics together with the decay rate of the inhibition determine the next firing time of  $F$ .

*The sensitivity of a depressing synapse to changes in cycle period contributes to maintain phase*

To illustrate the importance of a depressing synapse in maintaining phase, we compare the time courses of  $V_O$  and  $V_F$  for different cycle periods in the two cases where the synapse is depressing or non-depressing (Figure 3). Unless stated otherwise, we used one set of parameters that we referred to as the canonical model. The non-depressing synapse was modeled with the same equations, except that when  $O$  makes its burst  $s$  was set to a fixed value  $s_I$ , rather than the value of  $d$  (substitute  $s(0)=s_I$  in Equation 3). The value of  $s_I$  was chosen such that it matches the maximal value of  $s$  when the synapse is depressing and  $P = 275$ .

When the synapse was non-depressing,  $\Delta t$  remained fixed as  $P$  was increased (Figure 3A, bottom two pairs of traces). For the parameters used in Figure 3A,  $\Delta t$  was 250. At values of  $P$  smaller than  $\Delta t$ , the rhythm was disrupted ( $F$  did not burst) because  $O$  inhibited  $F$  before  $F$  could start a burst. When the synapse was depressing,  $\Delta t$  increased as  $P$  was increased (Figure 3B, bottom three pairs of traces). At low values of  $P$ , the rhythm was disrupted because the synapse was too weak ( $d$  did not sufficiently recover). We chose the maximal conductances of the depressing and non-depressing synapses so that at  $P = 275$ ,  $s$  and therefore  $\Delta t$  were identical for the two cases (compare third pair of traces in panels A and B).

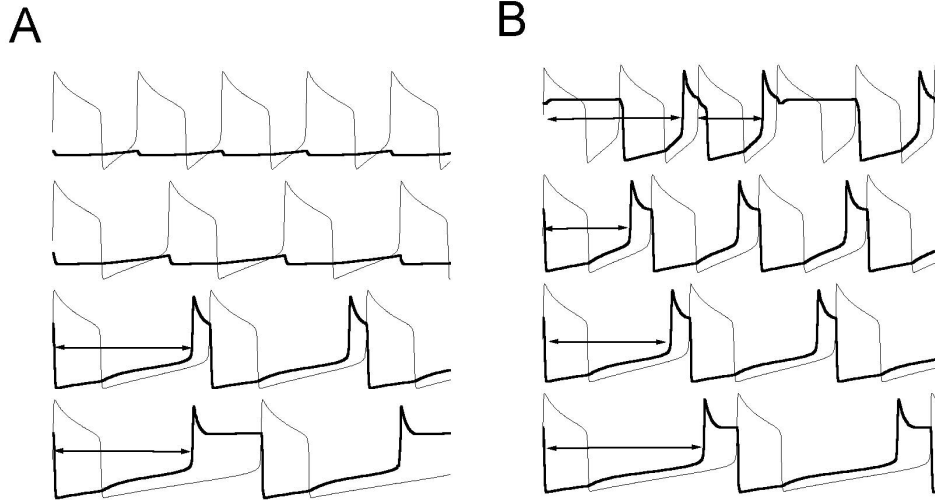


**Figure 3:** A depressing, but not a non-depressing, synapse increases the burst delay as period increases. Voltage traces of  $O$  (thin lines) and  $F$  (thick lines) for different  $P$  values (from top to bottom):  $P = 203, 235, 275$  and  $365$ . Arrows show the time interval between onset of burst in  $O$  and onset of burst in  $F$  ( $\Delta t$ ). **A.** Non-depressing synapse. For small values of  $P$ ,  $F$  does not burst (top two pairs of traces). For larger values of  $P$ ,  $\Delta t$  is constant (bottom two pair of traces) **B.** Depressing synapse. For small values of  $P$ ,  $F$  bursts every two cycles (top pair of traces; counted as disrupted bursts in the text). For larger values of  $P$ ,  $\Delta t$  increases as  $P$  increases (bottom three pair of traces).

*The effects of synaptic and intrinsic dynamics on the phase*

We saw that the time delay  $\Delta t$  is affected by the interaction between the intrinsic dynamics in  $F$  and the synaptic dynamics. In this section we examined the effects of different synaptic and intrinsic parameters of the model on the phasing of  $F$ , at different cycle periods (Figure 4). We changed the canonical model and studied the effect of the maximal synaptic conductance ( $g_{syn}$ , **A**), the time

constants of synaptic recovery ( $\tau_{\alpha}$ , **B**), synaptic decay ( $\tau_K$ , **C**) and intrinsic recovery variable in  $F$  ( $\tau_w$ , **D**).

The effect of decreasing  $g_{syn}$  was to lessen the effect of the inhibitory synapse. In particular, the value  $\tau_K$  became less relevant. Hence, with smaller  $g_{syn}$  values the size of the hump was reduced until it was eliminated,  $\phi$  was smaller and its dependence on  $P$  approached proportionality to  $1/P$ . Interestingly, for some  $g_{syn}$  values there was a range of  $P$  values where  $\phi$  was almost constant (for example, for  $g_{syn} = 0.6$ , and  $220 < P < 320$ ,  $\phi = 0.66$ . Figure 4A, thin line). In this range, any change in  $P$  results in a proportional change in  $\Delta t$ .

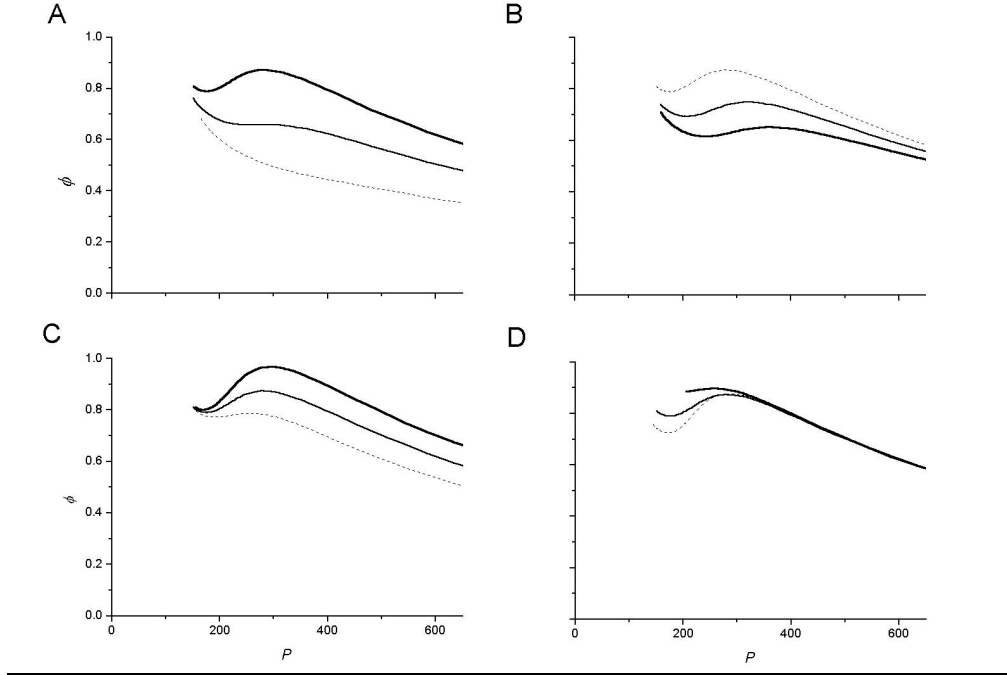


**Figure 4:** Effects of synaptic and intrinsic dynamics on phasing. **A.** The effect of the maximal synaptic conductance,  $g_{syn}$ : 0.5 (dotted line), 0.6 (thin line) and 0.7 (thick line, canonical). **B.** The effect of the time constant of recovery  $\tau_{\alpha}$ : 800 (dotted line, canonical), 1000 (thin line) and 1200 (thick line). **C.** The effect of the time constant of synaptic decay  $\tau_K$ : 400 (dotted line), 500 (thin line, canonical) and 600 (thick line). **D.** The effect of the time constant of intrinsic recovery in  $F$ ,  $\tau_w$ : 80 (dotted line), 100 (thin line, canonical) and 133 (thick line).

In Figure 4B we increased  $\tau_{\alpha}$  from the canonical value (dotted line). A larger  $\tau_{\alpha}$  value caused less recovery of the  $d$  variable for the same interburst duration in  $O$ . This effectively weakens the synapse and mimics the behavior seen with lowering  $g_{syn}$ . As in Figure 5A, this causes  $\Delta t$  to be smaller, and therefore  $\phi$  versus  $P$  becomes more proportional to  $1/P$  and the size of the hump is reduced. The hump also shifts to larger  $P$  values, because the synapse needs more time to recover to the strengths at which synaptic dynamics become important. At larger  $\tau_{\alpha}$  values, the hump is completely eliminated (not shown). When  $\tau_K$  was increased from its canonical value (Figure 4C, thin line), the size of the hump was increased. A larger  $\tau_K$  value caused less decay of the synapse during the interburst of  $F$ . This caused  $\Delta t$ , and hence  $\phi$ , to be larger. Opposite effects were seen when  $\tau_K$  was decreased from its canonical value.

Lastly, we changed the time constant  $\tau_w$  of the intrinsic recovery variable in  $F$ . When  $\tau_w$  was increased from its canonical value (Figure 4D, thin line), at  $P$  values lower than 275 the size of the hump was reduced but  $\phi$  was increased. With a larger  $\tau_w$ , the rate at which  $F$  evolved in its silent state was reduced and, as a result,  $\Delta t$  was increased. With slow intrinsic dynamics, even at low  $P$  values the relative contribution of the synaptic dynamics became significant, causing  $\phi$  to deviate from proportionality to  $1/P$ . At higher  $P$  values, the intrinsic dynamics did not play any role, and  $\phi$  was not affected.

## Discussion

How phase relations among components of a rhythmic neuronal network are maintained is still not understood. We propose a mechanism for promoting phase constancy that makes use of short-term synaptic depression. Using a simple biophysical model we showed that when an inhibitory synapse between an oscillator  $O$  and a follower neuron  $F$  is depressing, the phase relations depend on the cycling period  $P$ . If  $P$  is short relative to the time constant of synaptic recovery  $\tau_w$ , the synapse is too weak to delay the burst of  $F$  after the burst in  $O$  is terminated. In this case, the burst time of  $F$  is determined by its intrinsic dynamics. If the intrinsic dynamics in  $F$  are relatively fast,  $\Delta t$  (the time between  $O$  burst and  $F$  burst) is almost constant (independent of  $P$ ) and therefore the phase  $\phi(=\Delta t/P)$  is inversely related to  $P$ . If  $P$  is long relative to  $\tau_w$ , the synapse is strong and it maximally delays the burst of  $F$ . Again,  $\Delta t$  is independent of  $P$  and therefore  $\phi$  is inversely related to  $P$ . In an intermediate range of  $P$  values, however, an increase in  $P$  results in more recovery of the synapse. This leads to a larger increase  $\Delta t$ . As a result,  $\phi$  becomes less sensitive to  $P$ . We found that in some parameter ranges,  $\phi$  may become independent of  $P$  or even increase as  $P$  is increased. Hence the interaction between intrinsic and synaptic dynamics can contribute to the maintenance of phase, or at least to reduce the sensitivity of phase on period.

## References

- Cohen A, Ermentrout G, Kiemel T, Kopell N, Sigvardt K, Williams T (1992) Modelling of intersegmental coordination in the lamprey central pattern generator for locomotion. *Trends Neurosci* **15**: 434-438.
- Davis W (1969) The neural control of swimmeret beating in the lobster. *J Exp Biol* **50**: 99-117.
- Dicaprio R, Jordan G, Hampton T (1997) Maintenance of motor pattern phase relationships in the ventilatory system of the crab. *J Exp Biol* **200**: 963-974.
- Friesen W, Pearce R (1993) Mechanisms of intersegmental coordination in leech locomotion. *Semin Neurosci* **5**: 41-47.
- Grillner S (1981) Control of locomotion in bipeds, tetrapods and fish. In: Handbook of Physiology: The Nervous System (section 1)- Motor Control (Brooks U, ed), pp. 1179-1236. Bethesda: American Physiological Society.
- Hooper S (1997a) Phase maintenance in the pyloric pattern of the lobster (*Panulirus interruptus*) stomatogastric ganglion. *J Comput Neurosci* **4**: 191-205.
- Hooper S (1997b) The pyloric pattern of the lobster (*Panulirus interruptus*) stomatogastric ganglion comprises two phase maintaining subsets. *J Comput Neurosci* **4**: 207-219.
- Hume R, Getting P, Del Beccaro M (1982) Motor organization of *Tritonia* Swimming. I. Quantitative analysis of swim behavior and flexion neuron firing patterns. *J Neurophysiol* **47**: 60-74.
- Miller P (1966) The regulation of breathing in insects. *Adv Insect Physiol* **3**: 139-165.
- Morris C, Lécarré H (1981) Voltage oscillations in the barnacle giant muscle fiber. *Biophys J* **35**: 193-213.
- Pearson K, Iles J (1970) Discharge patterns of coxal levator and depressor motoneurone of the cockroach, *Periplaneta americana*. *J Exp Biol* **52**: 139-165.
- Nadim F, Manor Y, Nusbaum MP, Marder E (1998) Frequency regulation of a slow rhythm by a fast periodic input. *J Neurosci* **18**: 5053-5067.
- Williams T (1992) Phase coupling by synaptic spread in chains of coupled neuronal oscillators. *Science* **258**: 662-665.
- Young R (1975) Neuromuscular control of ventilation in the crab *Carcinus maenas*. *J Comp Physiol A* **101**: 1-37.

## Acknowledgments

This work was supported by ISF 314/99-1 (YM), NSF DMS-9973230 (AB, VB) and NIMH 60605-01 (FN).